An Experimental Investigation of Heat Transfer in the Post-Critical Heat Flux Regime

F.J. Munno
O.J. Sheaks
R.R. Smoker

April 1978

Department of Chemical and Nuclear Engineering
University of Maryland
College Park, Md. 20742

Prepared for
Argonne National Laboratory
Under Contract No. 31-109-38-3578

NOTICE

TABLE OF CONTENTS

ABSTRACT

A series of experiments were conducted to study the effect of voids in a heat removal medium (water) on the critical heat flux of a heater. The voids were created by permitting steam to flow through a diffusion plate below the heater. The void fraction was measured by use of a gamma densitometer. Incipient CHF was determined visually and CHF measured by monitoring the power flow into the heater. The results were correlated with the fluid flow resulting from the introduction of steam voids into the vessel. The correlation indicates that up to about 47% void the change in CHF is due to the change in the hydrodynamics of the system.

LIST OF FIGURES

LIST OF TABLES

I. Scope of Work

This report summarizes the work accomplished by the University of Maryland under a contract with Argonne National Laboratory entitled "Analytical and Experimental Investigations of Heat Transfer in the Post-Critical Heat Flux Regime." This work entailed an investigation of the effects of void content of a heat transfer fluid on the critical heat flux (CHF) of a heated element.

A vessel was constructed to contain heated water and an electrically heated element with provisions for admitting steam to control the void content. The current through the heater and the attendant voltage drop were monitored for each experimental run. The total void was measured, using a gamma ray transmission technique. The arrival of the departure from nucleate boiling or the passage of CHF into the unstable partial film boiling regime was noted visually, at which point the experimental run was terminated.

It had been hoped that an estimate of the difference in temperature between the heated element and the bulk fluid could be obtained by measuring the change in resistance of the heater with temperature. Difficulties in measuring the voltage drop and current to sufficient accuracy were encountered so that this data is not presented.

II. Introduction and Review of Literature

Following a sudden depressurization of a water cooled reactor, significant increases in the void content in the coolant would be expected. During the reflood, following the loss of fluid accident, high void fraction regimes would occur. This would give rise to changes in the heat transfer characteristics which could lead to increased temperatures in the fuel element. If the critical heat flux were achieved, the probability of fuel element disruption would increase significantly. It is important to measure this effect on the heat transfer properties so that designs may be deemed conservative.

Hsu and Graham[1] present an in-depth review of transport processes in two-phase systems. In addition to a rather complete discussion of correlations involving the boiling crisis in two-phase flow, they present excellent material covering the instrumentation useful in studying two-phase flow. They indicate that surprisingly good results can be obtained by making the simplest of assumptions:

1. The voids are homogeneously distributed.

2. There is no slip between the phases.

3. The system is in thermodynamic equilibrium and

4. The flow is at steady state.

These are indeed the assumptions which are made in the analysis of our data and the results are in good agreement with other published results.

In their discussion of flow patterns Hsu and Graham describe bubbly flow, slug flow, annular flow and mist flow. Of these, the present experimental system most closely approximates the description of bubbly flow - flow in which discrete bubbles are dispersed in a continuous flow of liquid. However, there is no net flow of fluid in our system, only a net flow of steam. Thus, the two-phase flow dynamics discussed are not immediately applicable.

In the excellent chapter on boiling crisis in two-phase flow, several correlations of CHF with void fraction were presented. These were all for significantly different geometries than that used in the present study and all assumed liquid flow with entrained void. Thus, no attempt was made to compare the present study data with any of these correlations.

V.I. Tolubinsky, et. at[2] studied what they termed "unsteady critical heat fluxes." In this study, power was supplied to a heating element so as to increase exponentially with time. They found that the time necessary to establish steady state boiling was short and decreased with increasing heat flux. Stainless steel or nickel tubes were used as heating elements. No effect of material on the critical heat flux was observed. They first attempted to determine the onset of the boiling crisis by means of visual observation, but found this to be unsatisfactory. They resorted to a bridge method of determining temperature by welding a nichrome wire to the test section. The results of their study indicate that heat fluxes exceeding CHF can exist in a heating element for a short time (0.5 to 0.8 micro-seconds) without significant surface overheating. This study tends to support our conclusion to ignore the effect of short transients that might cause the onset of the boiling crisis.

J. Kubie[3] conducted a study wherein he subjected a platinum wire heater to a stream of air bubbles. The experiment was conducted in such a manner that the air bubbles intersected the heater. The bubbles were 0.8mm, 1.6mm and 2.8mm in diameter. The frequency of bubble generation extended to include 40 bubbles per second. He concluded that heat transfer rates in nucleate boiling and in two-phase flow without change of phase are of the same order of magnitude. This leads to the conclusion that heat transfer is hydrodynamic in nature. He postulated that the bubble carried unheated water in its wake and that heat is transferred to this water by an unsteady state heat transfer process. Thus, transient conduction into the liquid phase becomes the most important heat transfer mechanisms. He estimates that this mechanism accounts for 75% of the total observed heat transfer. Of importance to our study is his observation that larger bubbles increase the forced convection heat transfer.

An analysis of critical heat flux in cross flow condition is presented by Lienhard and Eichhorn[4]. In this paper, they present a correlation of the onset of the boiling crisis as a function of the hydrodynamics of the heat transfer medium. There is excellent agreement between published heat transfer data and their theoretical development. This correlation will be presented in the conclusion of this report.

III. Description of Apparatus

The experiment was conducted in a two-section glass column (hereinafter referred to as the vessel) which was supported on a stable table with plywood back attached. (See Figure 1.) Steam and hot water feed lines entered the base of the vessel by means of a central connecting line. This connecting line also served as the drain for the vessel. The connecting line was tapped through an aluminum plate at the base of the vessel. The steam line had an orifice meter, a pressure gauge and an in-line temperature sensor integrated within it. The pressure drop across the orifice was measured by a manometer. The pressure in the steam line was monitored by a Reid vapor pressure gauge. The vessel consists of two glass columns, 15.3 cm inner diameter; the bottom section was 20 cm in length and the top section was 60 cm long. The base of the column was attached to a 38.5 cm square, 1.27 cm thick aluminum plate. The vessel was attached to the base plate with a snug fitting steel collar and a gasket. The feed/drain line was tapped through the aluminum plate and was positioned at the center of the column with an opening approximately 5 cm from the bottom of the vessel. This opening served as a nozzle which diverted the steam flow radially.

Figure 1. Schematic of Apparatus

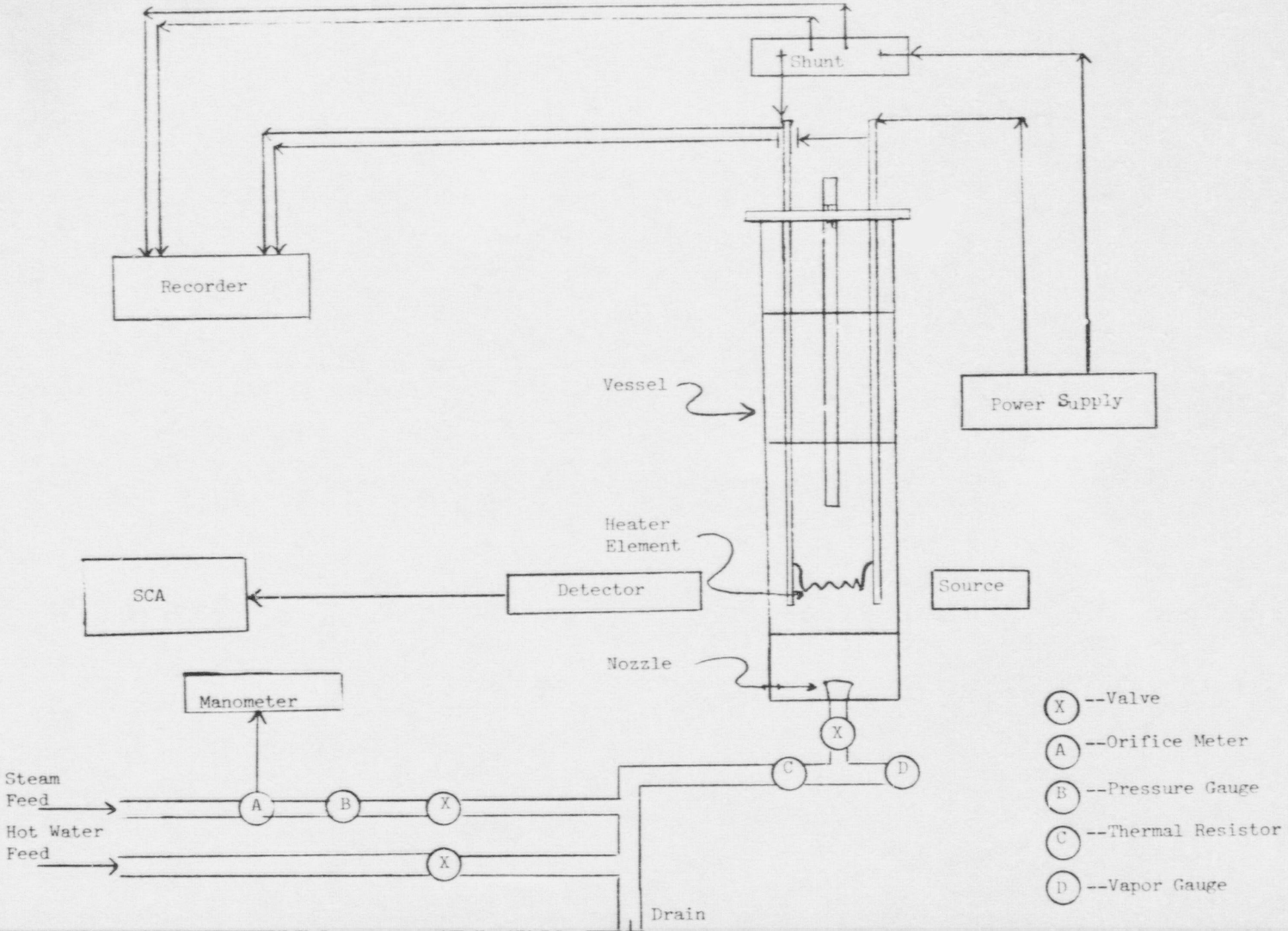

A diffusing plate made of aluminum was clamped between the two sections of the vessel. This plate had 100 holes, 0.159 cm in diameter, drilled in a square array one half inch on center and served to more evenly distribute the steam flow over the upper section which contained the heater. The top of the upper column had a 24 x 24 x 4 cm wood collar fitted over it This collar was used to support and vary the height of the heater assembly. Also attached to this support were two lucite disks with holes drilled to provide dampening of the motion of the agitated fluid.

The heating unit consisted of a single wire filament of approximately 21 cm in length, made of Advance (Constantin). The filament was secured at each end to a brass holder by means of a vise-like arrangement. The brass holders were silver soldered to the bottom of two 90 cm lengths of copper pipe. The electrical connections were made through these pipes by insulated ground straps connected to the voltage supply.

The power supply used was a standard D.C. arc welder. A 50 millivolt, 300 ampere shunt was connected in the circuit in series with the heater filament. The current and voltage drop across the heater were monitored by a linear recorder. Due to the range of the recorder used, a voltage divider was constructed for the voltage drop measurements. This led to problems of accuracy and reproducibility.

Void fraction measurements were made by employing a gamma densitometer. This consisted of a collimated 5 milliCurie source of Cobalt-60 which emits primary gamma rays at 1.17 MeV and 1.33 MeV, together with a collimated Sodium Iodine crystal, a single channel analyzer and associated electronics. The single channel analyzer was set up so as to count the uncollided photons; that is, the integral under the two photopeaks.

An orifice meter was constructed to measure the steam flow rate into the system. It was made of two stainless steel disks which were drilled and tapped to accommodate the steam line. Each of these stainless steel plates was also drilled and tapped along a radius for the pressure drop measurements. Aluminum tubing is used to connect this to the mercury manometer. A brass orifice plate with a 1.275 cm diameter orifice is clamped between the steel plates.

A list of the equipment used and specifications is provided in appendix A.

IV. Calibration of System Components

Prior to carrying out the experiment, various components of the system were calibrated to insure accuracy of the data.

The in-line thermal resistor in the steam line was calibrated by measuring the resistance of the element as a function of temperature in a heated mineral bath. The temperature of the bath was monitored by a standard 250°C thermometer over a range of 50°C to 210°C. A least squares fit was made to the data and this curve was later used to convert the measured resistance to an equivalent temperature. The least square fit was found to be linear over the range of interest.

The Advance* wire used for the filament was specified by the manufacturer to have a resistivity of 0.097 ohms/foot at 20°C. Measurement with a milliohmmeter verified this reading. Further verification of this value was obtained during a set of experiments to measure the contact resistance of the wire. This contact resistance was found to be of such a low value that the milliohmmeter was off-scale. Consequently, a set of experiments in which the length of the filament was varied and the voltage drop and current were recorded was carried out. These results are presented in Figure 2. The contact resistance was found to be 0.0027 ohms. This amounts to approximately 3% of the overall resistance and thus does not result in significant error in the measurement of CHF. The temperature of the wire during the run was assumed to be at 100°C since a measured value was not obtained. The resistance of each filament was corrected for this temperature.

A calibrated digital voltmeter was used to calibrate the voltage supply as measured by a chart recorder. Calibration curves were generated and used to convert chart recorder readings to actual values.

V. Procedure

A heater filament made of Advance was placed in the brass holder and secured. The length of the filament was 23.8 cm; 21.0 cm active length between the brackets and 1.4 cm on each end filled into the holder. The heater assembly was lowered into position and all electrical connections made (Figure 1). With the vessel still devoid of water, the gamma source was put into its collimator and a number of readings taken to establish an average count rate for 100% void fraction. Next hot water (80-90°C) was admitted into the vessel. The water height was usually selected so as to be approximately two

---

* Trade Name

Figure 2. Resistance (ohms) vs. Length of Filament (cm)

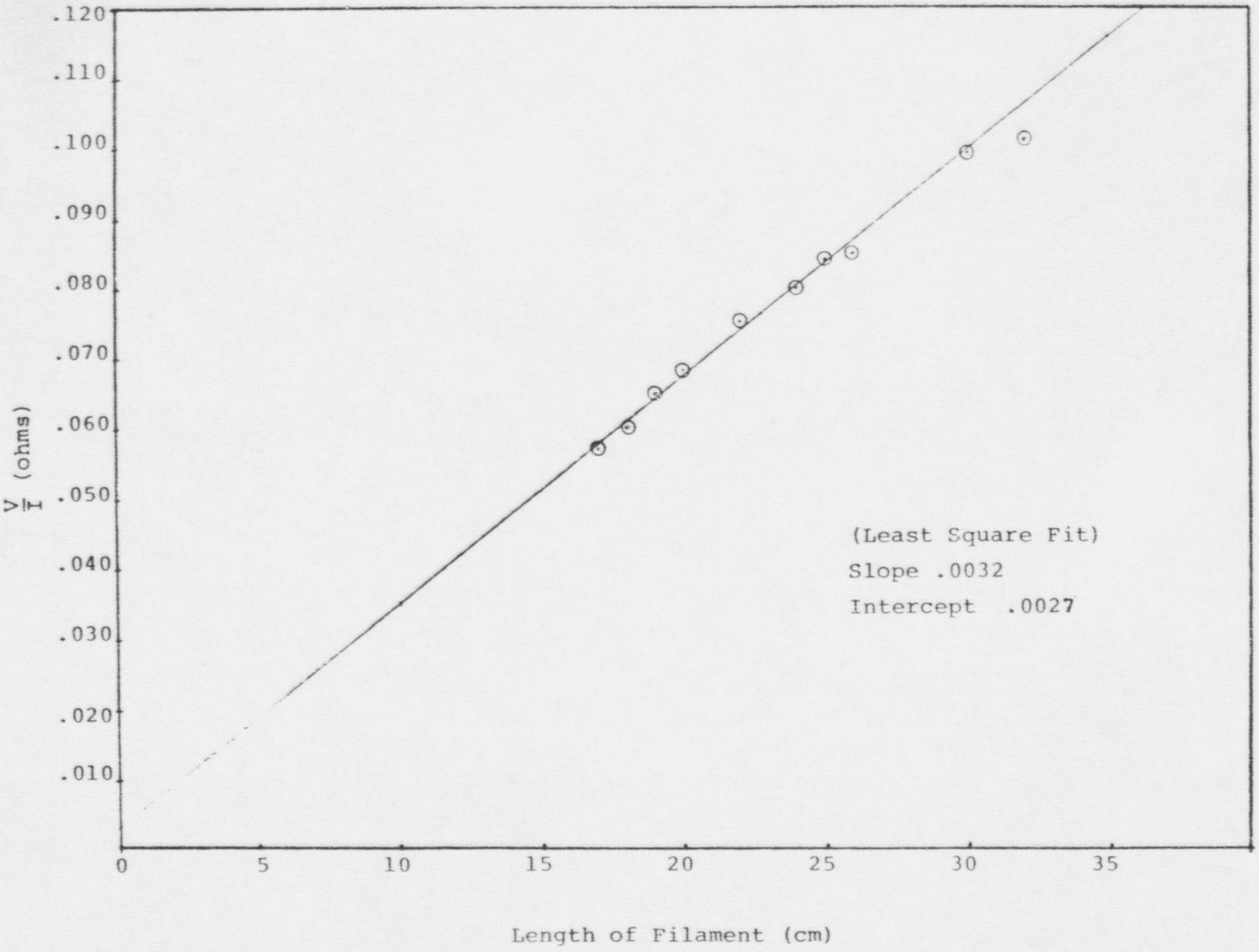

centimeters above the filament, although this varied from run to run. Steam was then made to flow through the lines and by-passed into the sewer to insure removal of any condensation in the steam line. The steam was allowed to pass into the vessel to heat the water to 100°C. The average count rate for the zero void fraction was then obtained. This procedure, together with the assumption of Beer's law, provided the calibration graph so that the average void content just below the filament could be determined.

Each run was performed as follows: Steam was admitted into the chamber. When the void fraction was stablized (this was ascertained visually together with the assumption that no steam will condense at 100°C in the vessel) voltage was applied to the filament and slowly increased until any portion of the filament passed the CHF as determined by visible glowing. The voltage applied to the filament was then immediately cut off. During the run, the voltage across the wire and calibrated shunt, the pressure drop across the orifice and the count rate of the gamma densitometer were recorded. The run was then repeated with a new steam flow rate. Periodically, water had to be drained out of the vessel as a buildup due to condensation did occur. Most of the data presented in this report is the result of using one filament. The ability to do this was gained through experience on the part of the operator.

VI. Results and Analysis

The data from two sets of runs entailing some 50 trails are presented in Tables I.A and I.B. The numbers recorded are for the data as recorded and converted, utilizing the calibration data. The resistance given is simply the ratio of the voltage measured to the current measured. The void fraction as measured ranged from about 5% to 47%, which was the highest achievable in this apparatus.

This data was then utilized to calculate the results as presented in Tables II.A and II.B. Note that the critical heat flux in most runs is approximately 500,000 BTU/ft^2-hr, which is in reasonable agreement with CHF for wires in pool boiling situations. However, it is necessary to note that this is the average heat flux of the filament when one area of the filament was observed to enter the film boiling regime. The length of wire actually involved in CHF would appear to be between one and two centimeters, but there was no way to measure this accurately in this experiment.

The procedure of creating voids by admitting steam in a jetting arrangement created a great deal of turbulence. Although this was a static system, patterns of swirling flow were created

Table IA. Measured Data-CHF vs. Void Fraction

Run #	Voltage (Volts)	Current (Amps)	Resistance (Ohms)	Void Fraction (%)	Steam Pressure (PSI)	Steam Temperature °F	Pressure Drop Across Orifice I_n H_g
1	8.75	126.6	.0691	5.39	59	303.8	.05
2	8.95	133.2	.0672	6.11	58	302.0	.05
3	9.08	134.4	.0676	6.22	59	305.6	.05
4	9.20	135.0	.0681	0.04	60	305.6	.025
*5	10.00	148.5	.0673	24.15	49	291.2	.085
*6	15.10	151.2	.0699	28.72	42	287.6	.15
7	12.08	174.6	.0692	26.28	40	278.6	.20
8	11.75	169.2	.0694	25.52	36	278.0	.15
9	12.25	175.8	.0697	20.26	44	282.2	.10
10	12.60	180.0	.0700	19.02	54	300.2	.05
11	12.15	174.0	.0698	19.02	59	307.4	.05
12	11.08	158.4	.0699	20.76	59	307.4	.05
13	12.00	171.6	.0699	4.82	59	307.4	.05
14	12.00	172.2	.0697	0.0	59	307.4	.05
15	11.75	168.6	.0697	27.54	44	287.6	.10
16	11.15	160.8	.0693	19.19	30	266.0	.25

Table IA. (cont.)

Run #	Voltage (Volts)	Current (Amps)	Resistance (Ohms)	Void Fraction (%)	Steam Pressure (PSI)	Steam Temperature °F	Pressure Drop Across Orifice $I_n H_g$
17	11.85	169.5	.0699	19.49	28	262.4	.25
18	11.60	166.8	.0695	19.93	28	260.6	.25
19	11.75	168.6	.0697	20.26	26	257.0	.275
20	11.95	171.0	.0699	20.03	24	255.2	.275
21	11.95	171.0	.0699	19.26	24	255.2	.275
22	12.00	171.6	.0699	21.42	20	248.0	.30
23	12.00	173.4	.0692	20.59	18	242.6	.35
24	11.40	162.6	.0701	5.62	59	305.6	.025
25	11.65	166.8	.0698	5.05	59	303.8	.025
26	11.53	165.9	.0695	7.16	59	305.6	.025
27	11.30	161.4	.0700	6.60	58	309.2	.025
28	11.65	167.1	.0697	5.81	59	305.6	.025
29	11.30	162.0	.0698	0	58	303.8	.025
30	11.00	158.4	.0694	0	58	305.6	.025
31	12.25	175.5	.0698	16.82	56	300.2	.025
32	12.00	172.5	.0696	17.29	56	300.2	.025

Table IA. (cont.)

Run #	Voltage (Volts)	Current (Amps)	Resistance (Ohms)	Void Fraction (%)	Steam Pressure (PSI)	Steam Temperature °F	Pressure Drop Across Orifice I_n H_g
33	12.52	179.1	.0699	24.44	45	287.6	.10
34	12.10	174.0	.0695	21.45	38	278.6	.15
35	12.13	174.0	.0697	20.76	34	275.0	.20

* Indicates burnout of filament.

Table IB. Measured Data-CHF vs. Void Fraction

Run #	Voltage (Volts)	Current (Amps)	Resistance (Ohms)	Void Fraction (%)	Steam Pressure (PSI)	Steam Temperature °F	Pressure Drop Across Orifice $I_n H_g$
1	12.35	177.0	.0698	33.46	32	271.2	.35
2	12.35	177.0	.0698	31.33	27	267.4	.35
3	12.08	174.0	.0694	39.27	14	241.3	.85
4	12.08	174.0	.0694	38.36	14	240.6	.85
5	12.03	172.5	.0697	29.82	54	308.5	.10
6	11.97	170.4	.0703	44.99	20	255.0	.75
7	12.03	172.2	.0699	44.63	22	256.8	.70
8	12.08	173.4	.0697	46.10	22	256.5	.70
9	12.08	173.1	.0698	45.64	18	250.0	.85
10	12.46	177.6	.0702	46.46	18	247.3	.90
11	12.46	177.6	.0702	45.33	18	248.5	.90
12	12.30	176.4	.0697	44.73	19	248.5	.90
13	12.67	181.8	.0697	46.89	20	252.7	.90
14	12.41	176.7	.0702	44.65	19	248.4	.90
15	12.51	179.1	.0698	46.08	19	249.1	.90
16	12.08	174.0	.0694	46.66	20	249.4	.90

Table IB. (cont.)

Run #	Voltage (Volts)	Current (Amps)	Resistance (Ohms)	Void Fraction (%)	Steam Pressure (PSI)	Steam Temperature °F	Pressure Drop Across Orifice $I_n H_g$
17	12.25	175.5	.0698	46.56	20	248.5	.85
18	12.08	173.4	.0697	45.71	20	249.1	.90
19	11.97	171.0	.0700	46.46	20	121.2	.90
20	12.51	178.5	.0701	48.39		121.2	.90

so that some net fluid flow was apparent. Very early in this effort, attempts were made to measure the local fluid velocities. One attempt involved the construction of a Pitot tube. The results were unsatisfactory, and therefore are not presented here. A decision was made to estimate the total flow rate by assuming that the net fluid flow rate in the vessel was equal to the flow rate of the steam in the vessel. The average flow rate of steam in the vessel was estimated by assuming that the orifice was ideal and using the following equation[5]

$$U_{bo} = C_o \frac{2 g_c (P_1 - P_2)}{\rho (1-\beta^4)} \qquad (1)$$

where

U_{bo} = steam flow in ft/sec

C_o = orifice constant

$P_1 = P_2$ differential pressure across orifice in lbs/ft^2

β = ratio of orifice diameter to pipe diameteter

g_c = gravatational constant (32.17 ft/sec^2)

From U_{bo}, and the cross sectional areas of the steam pipe and the vessel, the velocity of the steam in the vessel U_c, is calculated. The relative change in the heat transfer coefficient can thus be estimated by assuming it to be proportional to the Reynolds number, (hence U_{bo}).

VII. Conclusions

The results of Tables II.A and II.B are presented in the graph of Figure 3. Both the heat flux and the Reynolds number are plotted versus void fraction. The curves are fitted by eye to the points. The CHF appears to be increasing with void fraction. It seems to level off at about 30%. One may conjecture that it will decrease at some void percent greater than 50, however, there is no evidence presented in this data to support such a conclusion.

Figure 3. CHF and Re vs. Void Fraction

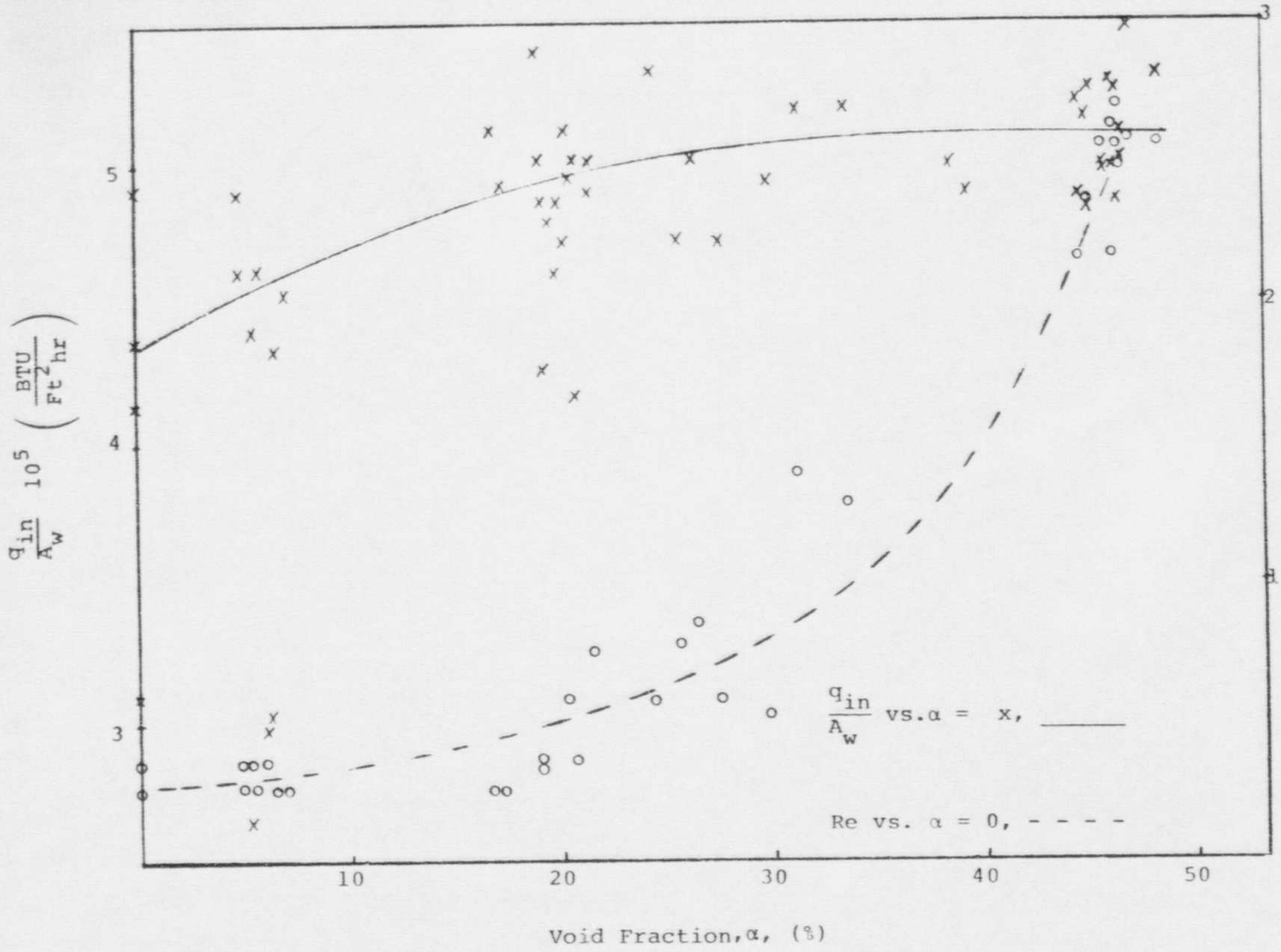

Table IIA. Results-CHF and Re vs. Void Fraction

Run #	Density (lbs/ft^3)	$P_1 - P_2$ (lbs/ft^2)	U_{bo} (ft/min)	U_c (ft/min)	$\frac{Q_{in}}{A_w}$ (BTU/ft^2-hr)	Void Fraction %	R_e
1	.0741	24.5	7029	48.82	519,800	33.5	129,100
2	.0636	24.5	7587	52.7	519,800	31.3	139,300
3	.0339	59.6	16,187	112.4	500,000	39.3	297,200
4	.0440	59.6	16,178	112.4	500,000	38.4	297,100
5	.0122	7.0	2,929	20.4	493,000	29.8	53,800
6	.0477	52.6	12,820	89.0	485,000	45.0	235,400
7	.0524	49.1	11,816	82.1	492,600	44.6	217,000
8	.0525	49.1	11,813	82.0	498,000	46.1	217,000
9	.0432	63.1	14,730	99.6	497,200	46.5	270,500
10	.0434	63.1	14,730	102.3	526,100	46.5	270,500
11	.0457	63.1	14,346	99.6	526,100	45.3	263,400
12	.0457	63.1	14,346	99.6	515,900	44.7	263,400
13	.0479	63.1	14,019	97.4	547,700	46.9	257,500

Table IIA. (cont.)

Run #	Density (lbs/ft^3)	$P_1 - P_2$ (lbs/ft^2)	U_{bo} (ft/min)	U_c (ft/min)	$\frac{Q_{in}}{A_w}$ (BTU/ft^2-hr)	Void Fraction %	R_e
14	.0458	63.1	14,344	99.6	521,400	44.6	263,400
15	.0457	63.1	14,352	99.7	528,500	46.1	263,600
16	.0481	63.1	13,984	97.1	500,000	46.7	256,800
17	.0482	59.6	13,582	94.3	511,200	46.5	249,400
18	.0482	63.1	13,981	97.1	498,000	45.7	256,700
19	.0481	63.1	13,994	97.2	486,700	46.5	257,000
20	.0481	63.1	13,994	97.2	531,000	48.4	257,000

Table IIB. Results-CHF and Re vs. Void Fraction

Run #	Density (lbs/ft^3)	$P_1 - P_2$ (lbs/ft^2)	U_{bo} (ft/min)	U_c (ft/min)	$\frac{Q_{in}}{A_w}$ (BTU/ft^2-hr)	Void Fraction %	R_e
1	.1346	3.5	1971.	13.7	276,500	5.4	36,200
2	.1329	3.5	1983.	13.8	297,500	6.1	36,400
3	.1342	3.5	1974.	13.7	304,600	6.2	36,200
4	.1366	1.8	1383.	9.6	310,000	0.04	25,400
* 5	--	--	--	--	---	--	--
* 6	--	--	--	--	---	--	--
7	.0936	14.0	4728.	32.8	501,500	26.3	86,800
8	.0840	10.5	4321.	30.0	472.700	25.5	79,300
9	.1027	7.0	3192	22.2	512,000	20.3	58,600
10	.1234	3.5	2058	14.3	539,300	19.0	37,800
11	.1338	3.5	1977.	13.7	502,700	19.0	36,300
12	.1338	3.5	1977	13.7	417,300	20.8	36,300
13	.1388	3.5	1977	13.7	489,600	4.8	36,300
14	.1338	3.5	1977	13.7	491,300	0	36,300

Table IIB. (cont.)

Run #	Density (lbs/ft^3)	$P_1 - P_2$ (lbs/ft^2)	U_{bo} (ft/min)	U_c (ft/min)	$\frac{Q_{in}}{A_w}$ (BTU/ft^2-hr)	Void Fraction %	R_e
15	.1018	7.0	3205.	22.3	471,000	27.6	58,900
16	.0710	17.5	6069.	42.2	426,300	19.2	111,400
17	.0665	17.5	6270.	43.6	477,600	19.5	115,200
18	.0667	17.5	6261.	43.5	460,100	19.9	115,000
19	.0622	19.3	6802	47.2	471,000	20.3	125,000
20	.0574	19.3	7076.	49.2	485,900	20.0	130,000
21	.0574	19.3	7076.	49.2	485,900	19.3	130,000
22	.0482	21.0	8065.	56.0	489,600	21.4	148,100
23	.0437	24.5	9153.	63.6	494,700	20.6	168,100
24	.1342	1.8	1396.	9.7	440,700	5.6	25,600
25	.1346	1.8	1394.	9.7	462,000	5.0	25,600
26	.1342	1.8	1396.	9.7	454,800	7.2	25,600

Table IIB. (cont.)

Run #	Density (lbs/ft^3)	$P_1 - P_2$ (lbs/ft^2)	U_{bo} (ft/min)	U_c (ft/min)	$\frac{Q_{in}}{A_w}$ (BTU/ft^2-hr)	Void Fraction %	R_e
27	.1311	1.8	1412.	9.8	433,600	6.6	26,000
28	.1342	1.8	1396.	9.7	462,900	5.8	25,600
29	.1322	1.8	1406.	9.8	435,300	0	25,800
30	.1318	1.8	1408.	9.8	414,300	0	25,900

The trend of increasing CHF with void fraction is probably attributable to the increased heat transfer brought about by the higher flow rates across the wire observed at these higher void fractions. As the void fraction increases still further, CHF remains practically independent of void fraction. This probably signifies a combination of factors. First, the heat transfer is increased due to increased flow rate. But second, and perhaps increasingly more important, the voids in the fluid are permitting less of the heater to be exposed to the fluid, thus decreasing the heat transfer area. That this is so is supported to some extent by the fact that only a small region of the heater is seen to pass through CHF at any time.

These conjectures can be illuminated by better instrumentation of the heater and a modified vessel and steam system. It was originally felt that by monitoring the change in the resistance of the filament during a run that the temperature could be ascertained. This assumption proved erroneous due to 1) the low temperature coefficient of resistivity of the filament used and 2) due to the fact that the large temperature change occurred locally and had only a small effect on the overall resistance of the heater. These problems may be circumvented by utilizing a platinum or tantalum heater instrumented with a number of thermocouples so as to get a temperature profile of the filament. The few attempts which were made with .010 inch diameter platinum wire lead us to believe that the melting point of platinum may be too low for this experiment, as in each case the wire melted through.

In order to further test the hypothesis the data were plotted versus the theoretical development and data presented by Lienhard and Eichhorn[4]. Since this correlation was for peak heat flux of cylinders in a cross flow, the correlation of Lienhard and Dhir[6] for peak pool boiling heat flux was used to determine an equivalent radius for our ribbon heater. The expression given is

$$\frac{q_{max,p}}{q_{max,z}} = 0.94/(R')^{1/4} \quad \text{for } 0.12 < R' \leq 1.17 \qquad (2)$$

where

$$q_{max,z} = \frac{\pi}{24} \rho_g^{1/2} h_{fg} \sqrt[4]{\sigma g(\rho_f - \rho_g)}$$

$$R' = \frac{R}{\sqrt{\frac{\sigma}{g(\rho_f - \rho_g)}}} \qquad (3)$$

ρ_f, ρ_g = saturated liquid and vapor densities

σ = surface tension between a saturated liquid and its vapor

g = gravitational acceleration

h_{fg} = latent heat of vaporization

By utilizing our data in expression (2) a value of R' was determined. Then from equation (3) R could be calculated. The values of the parameters used were

$\rho_f = 0.058$ g/cm^3

$\rho_g = 1.187 \times 10^{-3}$ g/cm^3

$\sigma = 58.9$ dynes/cm

$h_{fg} = 539.55$ calories/g

The value for R' was taken to be 0.701 cm and that for R as 0.176 cm.

The theoretical development in reference (4) gives an equation for "low-velocity" cross flows

$$\frac{\pi\, q_{max}}{\rho_g h_{fg} U_o} = 1 + \sqrt[3]{\frac{4}{\sigma/2R\rho_g U_o^2}} \qquad (4)$$

The data are presented in Figure 4. The points marked with Δ and ∇ are the results of the present study. We feel that the points represented by the ∇ were of such low velocity that a meaningful correlation did not exist. The rest of the data correlates well with the data presented for water in reference 4. The fact that it is at the lower limits of the data might be attributable to not taking slip into account between the steam stream and the water. Also, the flow was quite confused and turbulent due to the construction of the experiment. The steam was flowing through the system but there was obviously no net flow of water out of the vessel. Another source of error could be the assumption of an equivalent radius for the flat ribbon heater.

Figure 4. Peak Heat Flux Correlation

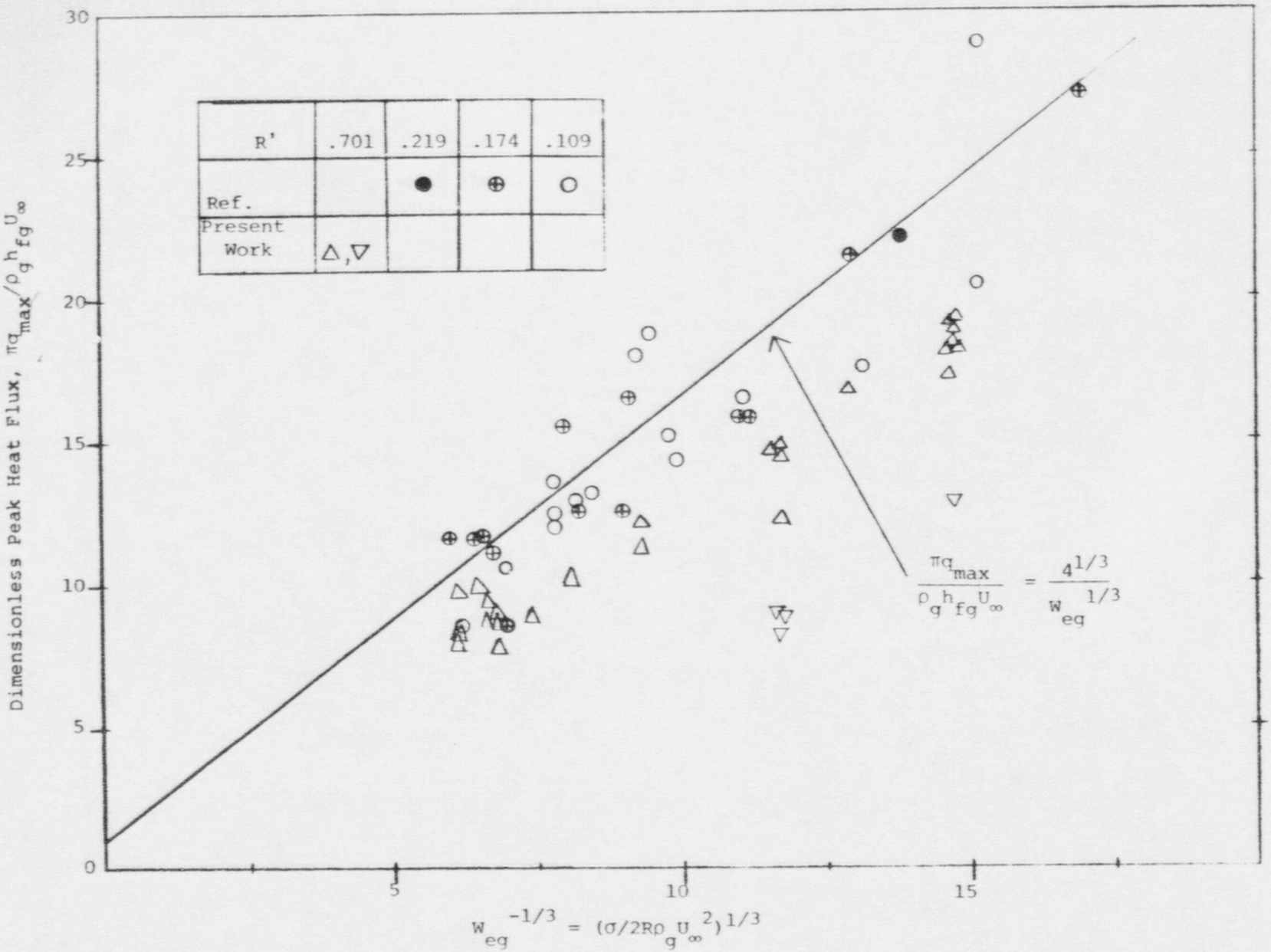

Thus to summarize, if further work in this area is contemplated, a flow system should be designed and a different type of heater with more instrumentation is necessary. The results obtained here would appear to show that during part of a blowdown the passage to CHF would occur at higher q/A and perhaps higher temperature than would occur in a static pool. For the range of void fraction studied here (<50%) the increase in CHF would appear to be primarily due to the change in hydrodynamics caused by the void flow as suggested by Kubie (3).

References:

1. Y.Y. Hsu and R.W. Graham, Transport Processes in Boiling and Two-Phase Systems, McGraw Hill Book Co., 1976.

2. V.I. Tolubinsky, et. al., "Investigation of Unsteady Critical Heat Fluxes", Heat Transfer, V.7, N.6, pp. 1-6, Nov. - Dec. 1975.

3. J. Kubie, "Bubble Induced Heat Transfer in Two Phase Gas-Liquid Flow", Int. J. Heat and Mass Transfer, V. 18, pp 537-551, Pergammon Press 1975.

4. J.H. Lienhard and R. Eichhorn, "Peak Boiling Heat Flux on Cylinders in a Cross Flow", Int. J. Heat and Mass Transfer, V. 19, pp 1135 - 1142, Pergammon Press, 1976.

5. C.O. Bennett and J.E. Meyers, Momentum, Heat and Mass Transfer, p. 45 , McGraw-Hill Book Co., Inc., 1962.

6. J.H. Lienhard and V.K. Dhir, Extended Hydrodynamics Theory of the Peak and Minimum Pool Boiling Heat Fluxes, NASA CR-2270, July 1973.

Appendix A

Equipment and Specifications

Power Supply

Arc Welder (Air Products)
Volts 208/230/460 Amps 44/40/20 Phase 1 Cycle 60
Rating: Amps 200 Volts D.C. 15/10/35
Type: RCHS
Style 483B101609
Open Circuit Voltage Low from 14 to 26
High from 23 to 35

Alternate Power Supply

Transitorized Power Supply (Try-Gon)
Model C 15-80 0-15 volts
0-80 amps

SCA Pack
Picker Cliniscaler

High Voltage Bias Supply
Tennelec, Model TC 941

Counter Timer
Tennelec, Model TC 545

Timing SCA
Tennelec, Model 544

Linear Amplifier
Tennelec, Model TC-203 BLR

Analog Ratemeter
Canberra, Model 6080

Appendix A (cont.)

Recorder, Chart, Two Pen
Linear Inc., Model 3

Detector
Picker, X-ray, Style 2802

Source
Cobalt 60, 5 mCi

Multimeter
Keithley, Model 172 Autoranging DMM

Standard Cell

Ohmeter
Shallcross, Model 673-D Multiohmeter

Wire Filament
Advance (Copper-Nickel Alloy)
R_0(20°C) .097 ohm/ft.

Thermal Resistor
Edison, 232N-90-2